Soil Dynamics and Earthquake Engineering 164 (2023) 107595

Contents lists available at ScienceDirect

Soil Dynamics and Earthquake Engineering

journal homepage: www.elsevier.com/locate/soildyn

Dynamic behavior of geocell-reinforced rubber sand mixtures under cyclic simple shear loading

Mengtao Wu [a,b], Wenhui Tian [a], Fangcheng Liu [a,*], Jun Yang [b]

[a] College of Civil Engineering, Hunan University of Technology, Zhuzhou, China
[b] Department of Civil Engineering, The University of Hong Kong, Pokfulam, Hong Kong

ARTICLE INFO

Keywords:
Geosynthetics
Cyclic simple shear loading
Rubber-sand mixture
Dynamic shear modulus
Damping ratio

ABSTRACT

Due to the attributes of low shear modulus and high initial damping, rubber sand mixtures (RSM) can be used as a soil alternative to reduce ground motions when seismic loads are of great concern. However, when RSM is used as a vibration isolation material for geotechnical seismic isolation systems, it suffers from a lack of load-bearing capacity. To overcome this, a three-dimensional interconnected geocell (one type of geosynthetics) is placed within RSM to increase the vertical confinement of the system. In this technical note, to investigate the shear modulus and damping ratio of geocell-reinforced RSM, large-scale cyclic triaxial tests were conducted on specimens prepared with four granulated rubber contents (by weight) and sheared under different cyclic shear strain amplitudes. The results show that Geocell reinforcement can restrict the development of local shear bands in the specimen, weaken the anti-S-shaped characteristics of hysteresis loops and enhance the damping ratio of RSM at large strain amplitudes. The tuck net effect causes an increase in the normal stress of both contact particles, and then leads to the degradation rate of the maximum shear modulus of RSM varying with the rubber content and vertical pressure. The normalized shear modulus degradation curves show the influence range of geocell reinforcement, and demonstrate that a rubber content of 20% for reinforced specimen may be an optimal value from the perspective of the stability of dynamic properties. Additionally, the quantitative analysis of the effect of geocell reinforcement on the mechanical behavior of RSM can provide a reference for subsequent theoretical research and engineering applications.

1. Introduction

With the development of the global automobile industry, the disposal of a large number of waste tires has become an increasingly serious environmental issue. Many studies have shown that scrap rubber obtained from the mechanical crushing of recycled tires can be widely used in civil engineering as an environmentally friendly material [1,2]. In particular, rubber-sand mixtures (RSM) composed of scrap rubber and natural sand in a certain proportion with low unit weight, strong deformation ability and high energy consumption, have been used in the fields of lightweight backfill [3], pipeline protection [4], embankment construction [5]. A complete list of summaries can be found in the work of Wu et al. [6]. Moreover, due to the frequent occurrence of seismic events, research on using RSM for seismic mitigation material has attracted increasing attention [7]. Of the outstanding contributions in this subject, Tsang et al. [8] first proposed replacing the site soil around the foundation of low-to-medium-rise buildings with RSM to form a dynamic soil-foundation-structure interaction (SFSI) system. The key advantage of the SFSI system is that seismic energy is dissipated before it transmits into the building, which improves the structural response under seismic loading [9]. In this case, it can not only allow for a significant consumption of recycled tires, but also considerably reduce the cost of building seismic isolation, and thus can be commonly applied to protect the structures in earthquake-prone areas, especially in developing countries.

Over the past two decades, the dynamic characteristics of RSM have been extensively investigated, to explore more beneficial manners of its application in soil dynamics and earthquake engineering. Feng and Sutter [10] conducted a resonant column test on granulated RSM, and demonstrated that the dynamic shear modulus gradually decreased with increasing the rubber content, while the damping ratio increased and the interaction between particles was enhanced. Shang et al. [11] studied the attenuation pattern of the dynamic shear modulus of granulated RSM under different consolidation pressures by using a cyclic

* Corresponding author.
E-mail addresses: cewu@hku.hk (M. Wu), tianwenhui198520@gmail.com (W. Tian), fcliu@hut.edu.cn (F. Liu), junyang@hku.hk (J. Yang).

https://doi.org/10.1016/j.soildyn.2022.107595
Received 25 May 2022; Received in revised form 26 September 2022; Accepted 12 October 2022
Available online 2 November 2022

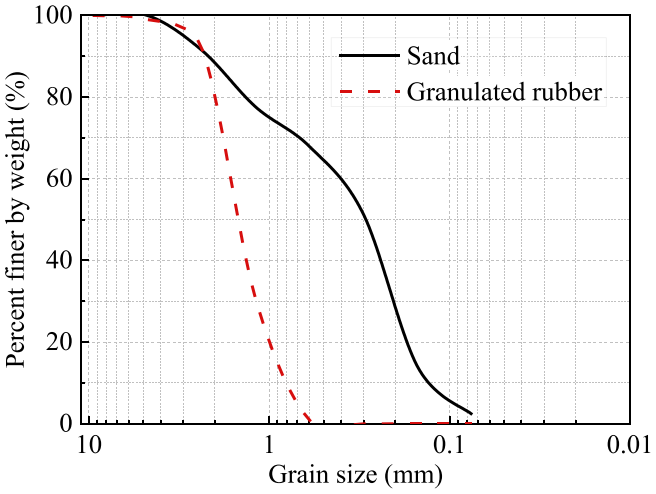

Fig. 1. Particle size distribution curves of sand and granulated rubber.

Table 1
The physical properties of sand and granulated rubber.

Materials	Specific gravity	Grain size (mm)	Mean size (mm)	Uniformity coefficient
sand	2.59	0.6–4.5	0.29	3.63
granulated rubber	1.21	0.07–2.3	1.5	2.24

simple shear test system. They found that the dynamic shear modulus of the mixtures increased with increasing consolidation pressure. Also, the existence of rubber effectively reduced the dynamic shear modulus, indicating the possibility of RSM as the seismic isolation material. Senetakis et al. [12] summarized the past and present high-amplitude resonant column test results, then proposed generic normalized shear modulus and damping ratio versus shearing strain amplitude curves, and finally derived the analytical expressions in terms of dynamic shear modulus and damping ratio of RSM under small strain conditions. Nakhaei et al. [13] performed a series of large-scale consolidated drained cyclic triaxial tests on granular soils mixed with granulated rubber under four confining pressures (50, 100, 200, and 300 kPa). They proposed an empirical relationship between confining pressure, rubber content, maximum shear modulus and normalized shear modulus. Anastasiadis et al. [14] studied the small-strain shear modulus and damping ratio of granulated RSM by torsional resonant column tests. The results showed that the response of the mixtures was strongly influenced by the rubber content and the relative size of rubber to sand particles. Anbazhagan et al. [15] investigated the dynamic response of mixtures in terms of confining pressure and rubber content in a range of small to large shear strain amplitudes. They found that for any percentage of tire crumb inclusion, the shear modulus increases and the damping ratio decreases with increasing confining pressure. Based on a series of dynamic hollow cylinder tests, Sarajpoor et al. [16] showed that the dynamic properties of sand-crumb rubber mixtures were mainly affected by the rubber content and confining stress values, while the relative density and rubber particle size were less effective in this regard. More related studies can be found in Liu et al. [17], Anbazhagan et al. [18], and Ding et al. [19].

As mentioned, the dynamic behavior of RSM with different particle sizes, rubber contents, stress states and test apparatuses has been paid attention in the literature. However, there is a lack of studies on the behavior of geosynthetic-reinforced RSM under repeated loads, which is the topic studied here. Due to RSM used as the seismic cushion is an approximately isotropic material, its shear modulus in both the horizontal and vertical directions is relatively small [20], which tends to increase the oscillating motion of the superstructure under seismic excitation. As a result, we believe that the introduction of geocell to reinforce RSM is an effective option. In this regard, the tuck net effect of three-dimensional geocell is used to improve the vertical modulus and lateral deformation resistance of RSM cushion, so as to enhance the seismic isolation performance and reduce the construction cost. Furthermore, the reinforced foundation usually exhibits higher ultimate bearing capacity and better settlement control, as well as appreciable resistance to liquefaction [21]. To the best knowledge of the authors, the behavior and mechanism of reinforced soils have been intensively studied [22,23], however, research on the mechanical properties, especially the dynamic behavior of geocell-reinforced RSM is still very

Table 2
Test conditions.

No.	Description	Value	Unit
①	Rubber content	0, 10, 20, 30, 50	%
②	vertical pressure σ_v	100, 200, 300	kPa
③	Shear displacement amplitude	2, 3, 4, 5, 6, 7, 8, 10	mm
④	Shear strain amplitude γ_a	0.01–0.06	–
⑤	geocell reinforcement	RSM, GCRSM	–

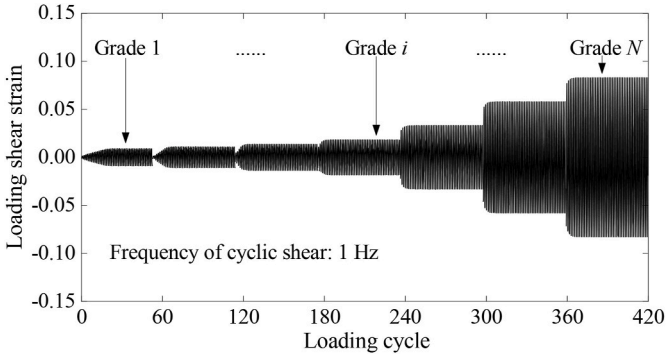

Fig. 3. Loading mode used in cyclic shear tests.

(a) sand and granulated rubber (b) HDPE geocell (c) Test apparatus

Fig. 2. Typical photos of test materials and equipment.

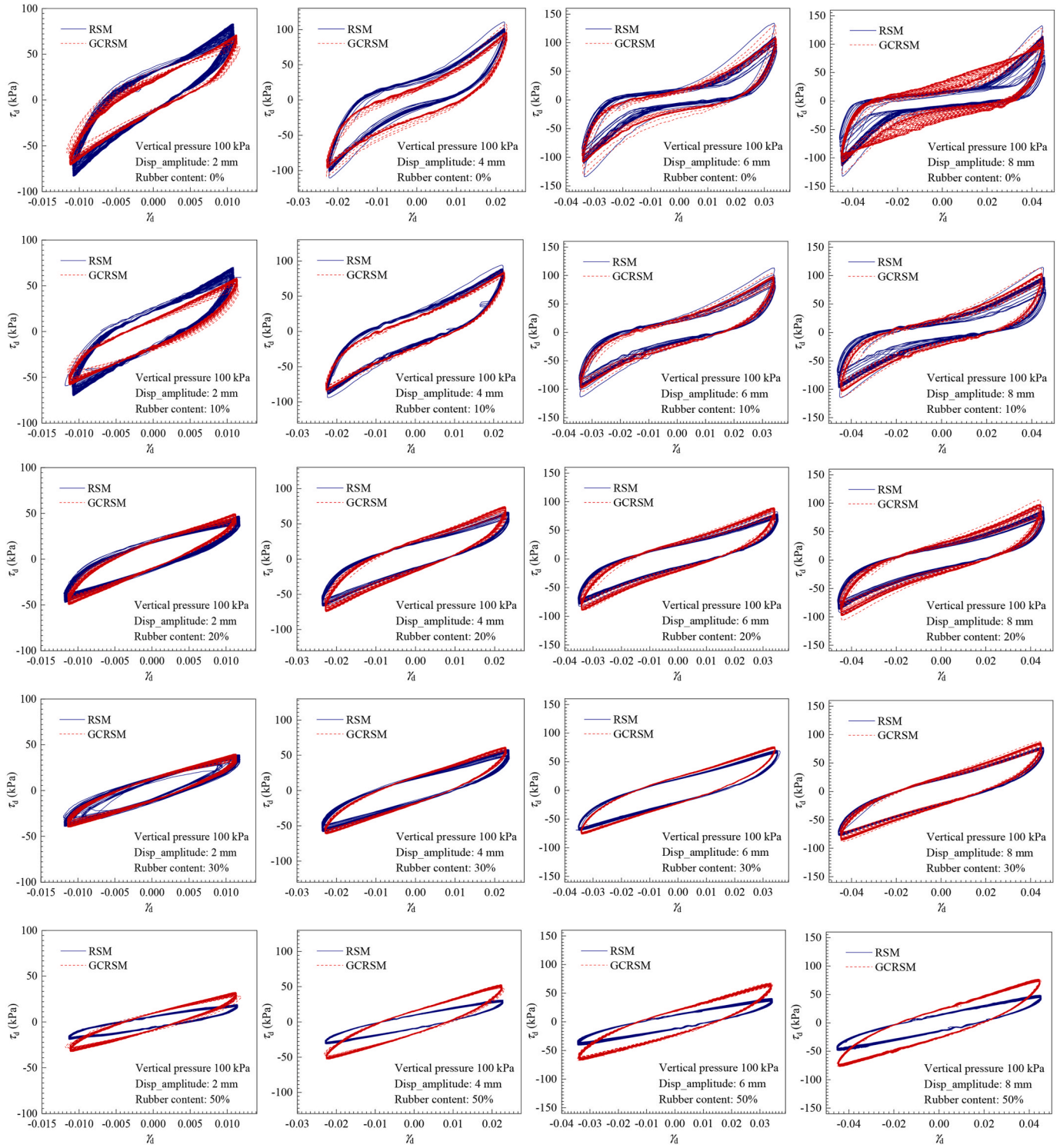

Fig. 4. Stress-strain curves of unreinforced and reinforced specimens (i.e., RSM and GGRSM) for confining pressure of 100 kPa with different percentages of rubber.

limited.

In this work, a series of large-scale cyclic simple shear tests were carried out to investigate geosynthetic reinforcement (with and without geocells), rubber content (0–50%), shear strain amplitude (0.01–0.06) and vertical pressure (100, 200, and 300 kPa) on the dynamic shear modulus and damping ratio of granulated RSM, and the empirical model of Darendeli was used to quantitatively evaluate the dynamic behavior of geosynthetic reinforced RSM. This research can provide a theoretical basis for the feasibility of geocell-reinforced RSM as a low-cost isolation cushion, which is conducive to the implementation of more rational reuse of waste tire rubber and the exploration of new methods for earthquake-resistant fortification.

2. Materials and testing methods

2.1. Test materials and equipment

Natural sand, scrap rubber and high-strength geocell were studied as

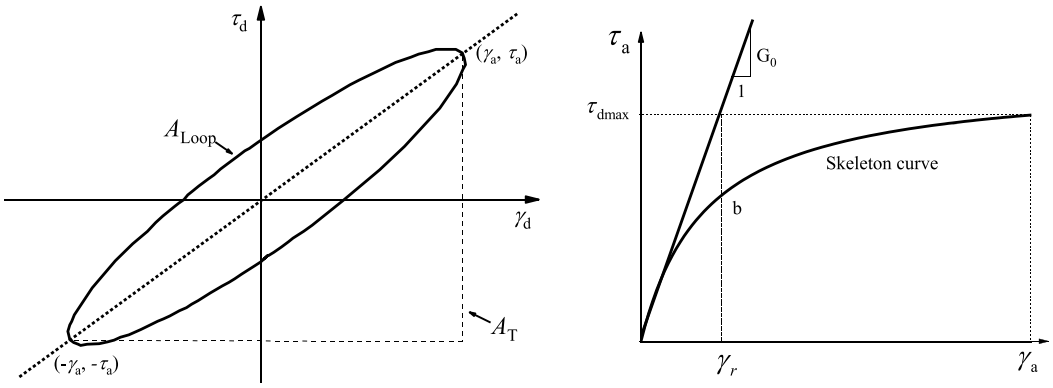

(a) hysteresis loop (b) skeleton curve

Fig. 5. Typical dynamic stress - strain curves of geotechnical material.

materials in this study. The sand originated from Hunan region, in central China, being a uniform quartz sand from the Xiangjiang River. The sand is classified as poorly graded sand according to the unified classification system (UCS). The rubber was procured from a local rubber processing factory and was classified as granulated rubber. It consists of scrap tires from which the steel and fibers have been removed. The grain size distribution of sand and granulated rubber is shown in Fig. 1 according to ASTM D 422–150 [24]. The physical properties of the two granular materials are listed in Table 1. The geocell used here was a high-density polyethylene (HDPE) material with mechanical properties characterized by: the tensile strength of approximately 18 MPa, welded joint strength of approximately 100 N/cm, cell height of 200 mm, welded joint spacing of 400 mm and cell thickness of 1 mm.

The cyclic simple shear test is recognized as one of the ideal laboratory methods for assessing soil dynamic characteristics, which can reproduce the dynamic stress-strain relationship of local sites during strong earthquakes and directly measure the dynamic shear modulus and damping ratio of soil medium [11]. In the present study, the test equipment was a large-scale cycle simple shear apparatus with a size of 700 mm in diameter and 200 mm in height. Layered circumferential four-point supporting steel rings and lined rubber film were used as shear boxes to provide lateral constraints for the specimens. The consolidated top plate was restrained by linear guide rails on the vertical column, to move up and down uniformly in the horizontal shear process of the specimens. Typical photos of the test equipment and material samples are shown in Fig. 2.

2.2. Test procedure

In this test, four types of RSM were considered, with 0%, 10%, 20%, 30% and 50% granulated rubber content by weight (i.e., mass of the rubber/total mass of the specimen). To ensure the comparability of test results, the same relative density was adopted for RSM specimens with different rubber contents. The following influencing parameters were of significant interest to the dynamic behavior of geocell reinforced RSM: (i) rubber content; (ii) vertical pressure; (iii) shear displacement amplitude (shear strain amplitude); and (iv) geocell reinforcement. The specific test conditions are listed in Table 2.

To obtain the dynamic characteristics of geosynthetic reinforced RSM in a certain range of strain amplitudes, a graded cyclic loading method was adopted to carry out the cyclic shear test. For each test condition, the same specimen was subjected to multi-stage loading from small to large displacement amplitudes, with 60 cycles at each loading level. In this case, the presented procedure is economical and feasible for testing the dynamic behavior of large-size specimens. The loading mode was set to a bidirectional equal amplitude sine wave with a frequency of 1 Hz, and the loading control displacement sequence is shown in Fig. 3. During horizontal cyclic shearing, the vertical pressure was remained constant.

3. Results and analysis

3.1. Hysteresis loops

Fig. 4 shows the hysteresis loops obtained from large-scale cyclic shear tests of unreinforced and reinforced specimens (i.e., RSM and GGRSM) for vertical pressure of 100 kPa with different percentages of rubber. The effects of rubber content and geocell reinforcement can be noticed by significant changes in hysteresis behavior.

When the rubber content is 0% (pure sand), the hysteresis loops of the unreinforced RSM exhibited a clear anti-S-shaped feature (i.e., the tangent slope of hysteresis loops near the stress change sign suddenly decreased and maintained increasing slowly, and increased sharply before the strain turning), and the anti-S-shaped feature became more evident with the increase of strain amplitude. This phenomenon is similar to cyclic mobility in conventional soil at large strain amplitudes, which is generally believed to be caused by shear bands in geotechnical media (e.g., see Vucetic [20]). At the same strain amplitude, the anti-S-shaped feature for GCRSM was significantly weaker than that for RSM, which indicates that the geocells inhibited the formation of shear bands. With increasing rubber content, the anti-S-shaped feature of the hysteresis loops gradually disappeared, and the difference in the shape of hysteresis loops between the RSM and GCRSM decreased. This is due to the good elasticity of granulated rubber buffering the bypassing and rolling of sand particles in the shearing process, which delays the development of shear bands.

For a lower rubber content, the slope of the hysteresis loops of GCRSM was essentially the same as that of RSM, or even slightly smaller than that of RSM. As the rubber content increased, the slope of the hysteresis loops of GCRSM increased significantly compared with that of RSM. The above characteristics can be explained as follows: when the rubber content is low, the sand-sand contact is the main force transfer path. After the geocells are added, a part of the sand-sand force transfer path is blocked by the cell plate, which leads to a decrease in the shear stiffness of GCRSM compared with that of RSM. With increasing of rubber content, the sand-rubber and rubber-rubber contacts increase, and the overall shear stiffness of RSM decreases. Once the geocell is added, the normal stress and the resistance required to overcome the relative displacement between the particles increase, resulting in a macroscopic enhancement of the shear stiffness of GCRSM compared with that of RSM.

In addition, the variation of the hysteresis loops with the number of cycles was generally smaller for GCRSM than for RSM at the same strain amplitude. With increasing rubber content, the difference between the

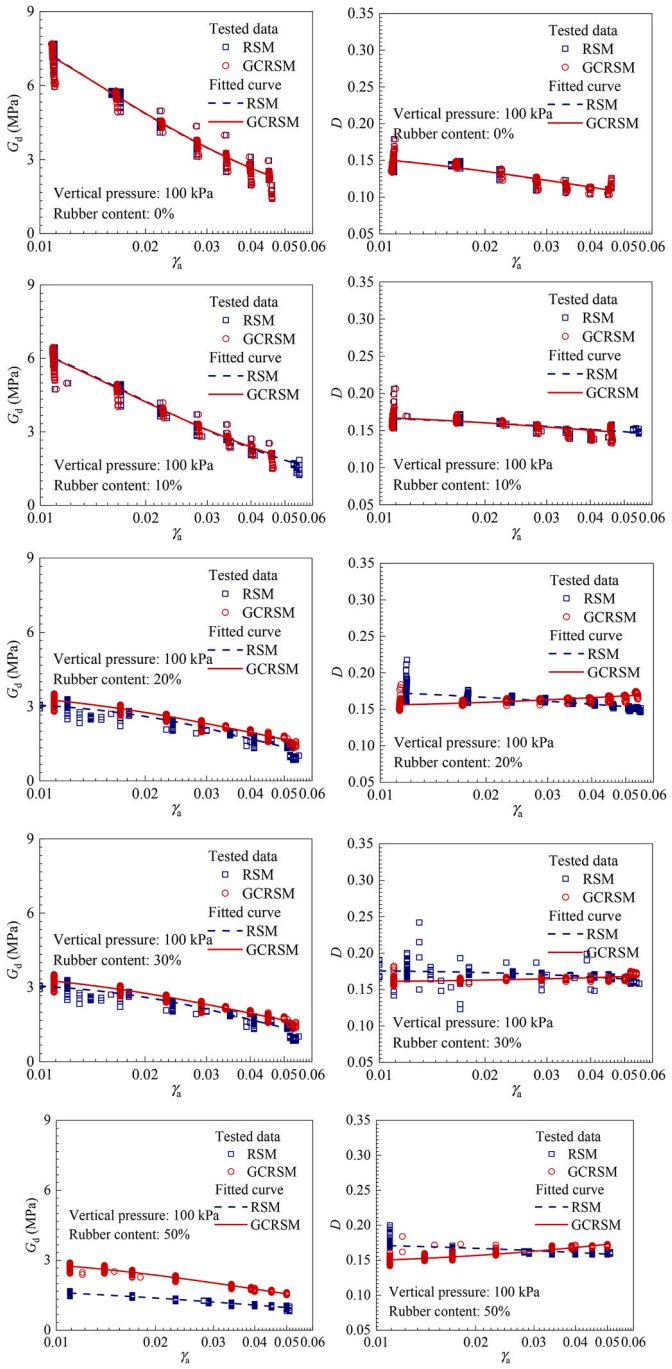

Fig. 6. Variation in the dynamic shear modulus and damping ratio of RSM and GCRSM with shear strain amplitude.

hysteresis loops of GCRSM and RSM with the number of cycles decreased. This is due to the fact that the dynamic properties are affected by cycling from the rearrangement of the force transfer skeleton in the specimen with the loading. More specifically, compared to typical RSM (e.g., see Liu et al. [17]), the inclusion of geocell constrains the rearrangement of contact particles on the force transfer skeleton, resulting in a reduced influence of the GCRSM with respect to the RSM by the number of cycles.

3.2. Dynamic shear modulus and damping ratio

According to the typical dynamic stress - strain curves of geotechnical materials shown in Fig. 5, the dynamic shear modulus and damping ratio can be calculated by Eqs (1) and (2).

$$G_d = \tau_\alpha / \gamma_\alpha \tag{1}$$

$$D = A_{Loop} / (\pi A_T) \tag{2}$$

where G_d is the dynamic shear modulus, D is the damping ratio; τ_α and γ_α are the shear stress and shear strain, respectively; and A_{Loop} and A_T are the area surrounded by the hysteresis loops and the area of the dotted triangle, respectively.

Fig. 6 shows the variation in the dynamic shear modulus and damping ratio of RSM and GCRSM with shear strain amplitude for different percentages of rubber at a vertical pressure of 100 kPa. For the same strain amplitude, the spatial distribution of the tested data of GCRSM was more concentrated than that of RSM, which indicates that the dynamic characteristics of RSM were less affected by the cyclic loading times due to geocell reinforcement. With the increase of rubber content, the difference between the dynamic characteristics of RSM and GCRSM affected by the cyclic loading times also decreases.

The empirical model of Darendeli [25] can be used to quantitatively evaluate the dynamic behavior of RSM and GCRSM, as shown in Eq. (3) ~ (9).

$$G_d = \frac{G_{dmax}}{1 + \left(\gamma_a / \gamma_{a,ref}\right)^\alpha} \tag{3}$$

$$D = b\left(\frac{G_d}{G_{dmax}}\right)^{0.1} D_{masing} + D_{min} \tag{4}$$

$$D_{masing} = c_1 D_{masing,\alpha=1.0} + c_2 D^2_{masing,\alpha=1.0} + c_3 D^3_{masing,\alpha=1.0} \tag{5}$$

$$D_{masing,\alpha=1.0}(\%) = \frac{100}{\pi}\left[4\frac{\gamma_a - \gamma_{a,ref}\ln\left(\frac{\gamma_a+\gamma_{a,ref}}{\gamma_{a,ref}}\right)}{\frac{\gamma_a^2}{\gamma_a+\gamma_{a,ref}}} - 2\right] \tag{6}$$

$$c_1 = -1.1143\alpha^2 + 1.8618\alpha + 0.2523 \tag{7}$$

$$c_2 = 0.0805\alpha^2 - 0.0710\alpha + 0.0095 \tag{8}$$

$$c_3 = -0.0005\alpha^2 + 0.0002\alpha + 0.0003 \tag{9}$$

where G_{dmax} is the maximum shear modulus; $\gamma_{a,ref}$ is the reference shear strain amplitude; α is an attenuation parameter of the modulus curve; D_{masing} denotes the damping ratio expected by the Masing hysteresis criterion; D_{min} denotes a small strain damping ratio; and b is a fitted parameter of the damping ratio curve.

The fitted values of the dynamic characteristics of RSM and GCRSM with different rubber contents and different vertical pressures are listed in Table 3, and the fitting curves of the dynamic characteristics at a vertical pressure of 100 kPa are shown in Fig. 6. The comparison results are shown as follows: 1) When the rubber content was low (less than 10%), the $G_d \sim \gamma_a$ curves and $D \sim \gamma_a$ curves of RSM and GCRSM generally coincided with each other, and geocell reinforcement had little effect on the dynamic shear modulus of RSM. 2) When the rubber content reached 20%, the $G_d \sim \gamma_a$ curves of GCRSM were higher than those of RSM, especially for high percentages of rubber. 3) When the rubber content reached 20%, the $D \sim \gamma_a$ curves of GCRSM and RSM were crossed. For γ_a <0.03, the damping ratio of GCRSM was slightly smaller than that of RSM. While for γ_a >0.03, the damping ratio of GCRSM was evidently larger than that of RSM. 4) Within the strain amplitude range studied in this paper, the damping ratio of RSM decreased with increasing of shear strain, while the opposite was true for GCRSM.

Table 3
Fitted parameters of the dynamic characteristic curves of RSM and GCRSM.

Vertical pressure (kPa)	Parameters	RSM					GCRSM				
		0%	10%	20%	30%	50%	0%	10%	20%	30%	50%
100	G_{dmax} (MPa)	12.64	8.876	5.584	3.275	1.998	11.98	9.447	5.411	3.806	3.311
	$\gamma_{a,ref}$	0.014	0.019	0.023	0.042	0.047	0.015	0.017	0.03	0.042	0.045
	α	1.23	1.37	1.037	1.841	0.93	1.266	1.261	1.179	1.326	1.122
	b	−0.191	−0.068	−0.135	−0.045	−0.134	−0.183	−0.089	0.08	0.043	0.197
	D_{min}/%	17.482	17.281	18.335	17.652	17.659	17.238	17.683	15.07	15.936	14.17
200	G_{dmax}/MPa	13.96	11.61	9.522	5.976	3.541	10.38	8.372	9.67	6.493	5.176
	$\gamma_{a,ref}$	0.028	0.025	0.029	0.04	0.055	0.038	0.043	0.029	0.042	0.051
	α	1.456	1.221	1.319	1.147	1.122	1.889	1.579	1.093	1.066	1.067
	b	0.012	−0.019	0.058	0.009	0.008	0.209	0.064	0.111	0.164	0.241
	D_{min}/%	12.574	14.646	14.278	16.501	14.714	9.66	13.712	13.565	13.591	12.318
300	G_{dmax}/MPa	16.19	12.05	13.27	8.18	4.982	12.91	11.65	11.39	8.107	4.993
	$\gamma_{a,ref}$	0.037	0.038	0.025	0.039	0.056	0.046	0.041	0.036	0.046	0.065
	α	1.547	1.42	1.002	1.15	1.037	1.659	1.178	1.204	1.011	1.019
	b	0.174	0.139	0.181	0.126	0.019	0.168	0.057	0.116	0.12	0.16
	D_{min}/%	8.509	10.545	12.122	13.872	14.005	10.06	13.573	12.899	14.075	12.379

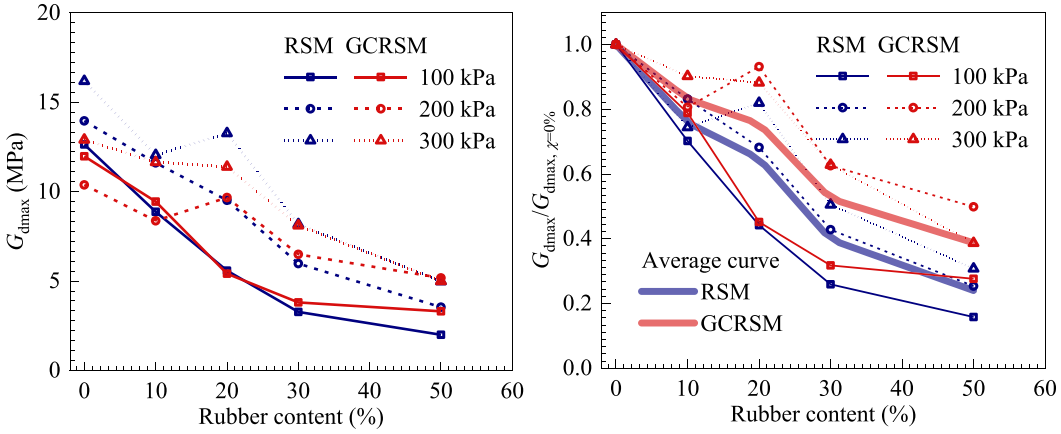

Fig. 7. Variation in the maximum shear modulus G_{dmax} and the normalized shear modulus $G_{dmax}/G_{dmax,\chi=0\%}$ of RSM and GGRSM versus the rubber content.

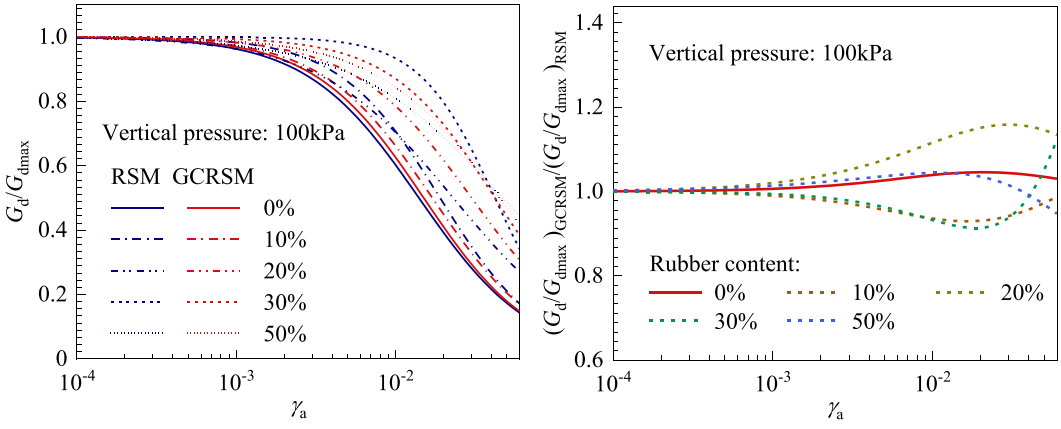

Fig. 8. Variation in normalized shear modulus G_d/G_{dmax} and $(G_d/G_{dmax})_{GCRSM}/(G_d/G_{dmax})_{RSM}$ of RSM and GGRSM versus the shear strain.

3.3. Normalized shear modulus degradation curves

Fig. 7 shows the degradation curves of the maximum shear modulus G_{dmax} and the normalized shear modulus $G_{dmax}/G_{dmax,\chi=0\%}$ of RSM and GCRSM varying with the rubber content, where $G_{dmax,\chi=0\%}$ is defined as the dynamic shear modulus of 0% RSM (i.e., pure sand). With increasing rubber content, one can find that the G_{dmax} curve decreased exponentially with the degradation rate being first fast and then slower. Meanwhile, the increase in vertical pressure accelerated the degradation rate of the $G_{dmax}/G_{dmax,\chi=0\%}$ curve. Comparing the degradation curves of RSM and GCRSM at different vertical pressures, it was noticed that the degradation rate of the former is slower than that of the latter.

Fig. 8 further shows the degradation curves of the normalized shear modulus G_d/G_{dmax} and $(G_d/G_{dmax})_{GCRSM}/(G_d/G_{dmax})_{RSM}$ of RSM and GCRSM varying with the shear strain. Since the shear strain amplitudes designed in the presented test procedure fall within a large strain range, smaller to 0.01% strain levels are extrapolated through the Darendeli model. The difference between the G_d/G_{dmax} curves of GCRSM and RSM

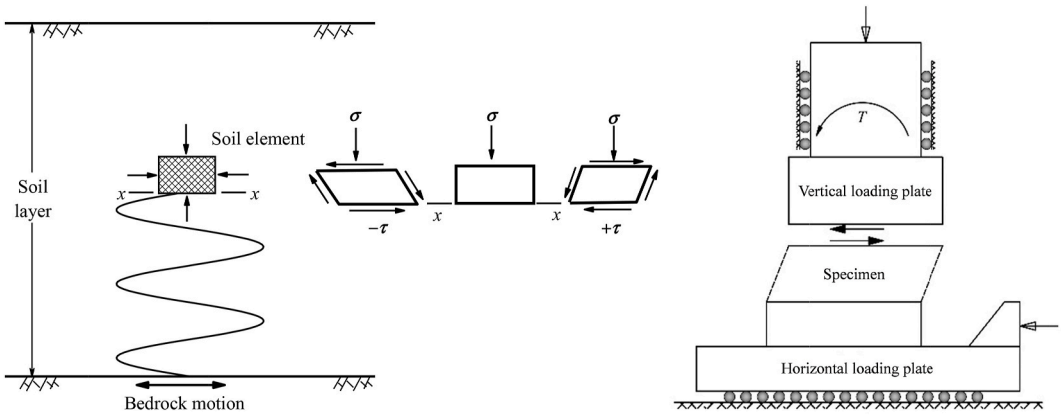

Fig. 9. (a) Stress-strain state of a soil element subject to seismic loading (left), (b) Deformation control of soil specimens during cyclic shear (right).

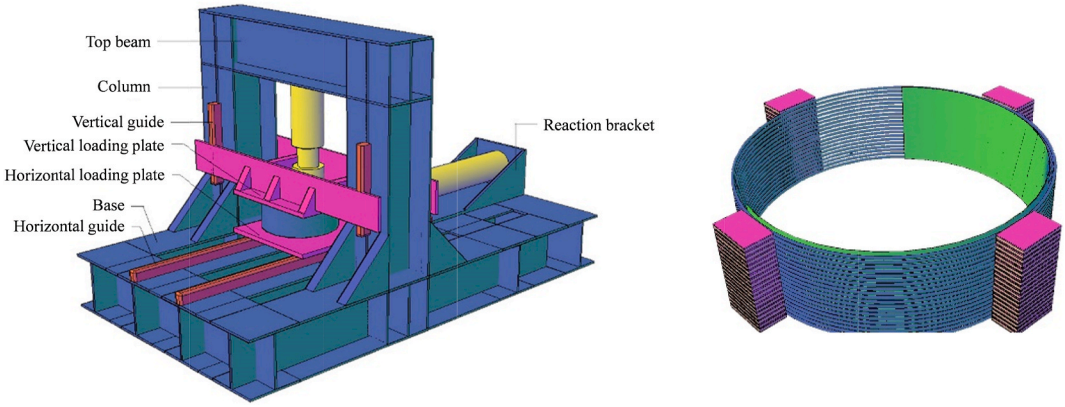

Fig. 10. Construction of (a) the developed large-scale shear apparatus (left) and (b) the designed large shear box (right).

with the same rubber content was small, especially for the strain amplitudes less than 10^{-3}, which almost overlapped. At a vertical pressure of 100 kPa, the normalized value of $(G_d/G_{dmax})_{GCRSM}/(G_d/G_{dmax})_{RSM}$ was between 0.9 and 1.18 in the strain range of 10^{-4} to 10^{-1}, which indicates that the influence of geocell reinforcement on the normalized shear modulus degradation curves was significant up to 20% rubber content.

4. Discussion

As shown in Fig. 9a, the main characteristics of the stress-strain state at an arbitrary point of the soil layer in a free field are as follows. (i) Horizontal shear deformation of the soil element always occurs in the laterally constrained consolidation state. (ii) Vertical deformation of the soil element caused by shear expansion or shear contraction can occur during cyclic shear. (iii) Top surface of the soil element always remains horizontal during cyclic shear according to the assumption of layered site. The ideal cyclic simple shear test equipment is required to be capable of achieving the above deformation control applied to a specific specimen (see Fig. 9b).

For conventional cyclic simple shear test equipment, the lateral boundary stiffness of the vertical loading plate can be easily guaranteed because the specimen size is usually small (e.g., 70 mm in diameter and 20 mm in height) and the torsional moment generated by cyclic shear is relatively low. As the specimen size increases (e.g., 700 mm in diameter and 200 mm in height in this paper), the torsional moment increases exponentially. Therefore, it is a key challenge to ensure that the vertical loading plate can be freely displaced, while maintaining sufficient resistance to torsional stiffness in the vertical plane. For this reason, the authors' team has designed a large-scale cyclic simple shear test apparatus, as shown in Fig. 10a. In the developed apparatus, the vertical/horizontal loading plates located at the top and bottom of the specimen are constrained by a series of linear guides so they can be translated vertically/horizontally. The shear box containing the specimen consists of layered steel rings, which are interlaced with the rubber membrane at four discontinuous load-bearing lugs (see Fig. 10b). These features of the equipment ensure that the appropriate boundary conditions for the soil specimens during testing are similar to those of the soil elements at the seismic site. The test results for reinforced and unreinforced RSM showed that the dynamic stress-strain relationships obtained from the large-scale cyclic simple shear tests reflect well the hysteretic, nonlinear and ratcheting properties of the mixtures under cyclic loading. With these findings, the prevailing mechanism can be interpreted as follows.

Overall, the reinforcement mechanism of the geocell with granular material is mainly reflected in the tuck net effect. The lateral deformation of the medium due to vertical pressure leads to tightening of the geocell sheet, and the corresponding reaction force increases the confining pressure of the medium and the normal stress of both contact particles. As a result, the resistance required to overcome the movement between the particles during the cyclic shear process, which is manifested as an increase in the shear modulus on a macro level. In addition, with the increase of the rubber content, the shear modulus of RSM decreases and the potential of lateral deformation increases, resulting in a more substantial tuck net effect of geocell and a more pronounced improvement in the dynamic shear modulus.

When the shear strain amplitude is relatively low, the particle contacts in reinforced RSM become closer due to the additional confining pressure generated by the tuck net effect of the geocell. This leads to the increase of force transfer paths between particles and the decrease of

losses during energy propagation, thus the damping ratio of reinforced RSM is slightly less than that of unreinforced RSM. When the shear strain amplitude is relatively large, the unreinforced RSM tends to generate shear bands (deformation localization is one of the important features in the large-strain of soils [26]). The granular materials involved in energy dissipation by friction effect are mainly limited within the shear band zones, thus the damping ratio has a reduction trend with increasing of shear strain amplitude. Meanwhile, the reinforcement of the geocell delays the development of deformation localization in the specimen, allowing the sand and granulated rubber within the entire specimen height to still participate in the energy dissipation, thus the damping ratio can continue to increase with increasing shear strain amplitude.

5. Conclusion

In this paper, the dynamic behavior of geocell-reinforced RSM under repeated loads were studied by large-scale cyclic shear tests, and the effects of rubber content, vertical pressure and strain amplitude on dynamic shear modulus and damping ratio were discussed. The following conclusions are drawn: 1) The addition of geocell in RSM restricted the development of shear bands and caused shear deformation to occur uniformly in the entire specimen height, which weakened the anti-S-shaped feature of hysteresis loops of RSM at large strain amplitudes and full the shape of hysteresis loops, so that the damping ratio of geocell reinforced RSM always increased with the increase of shear strain amplitude. 2) Geocell effectively restrained the relative displacement of particle contacts in the force transfer skeleton of RSM during the cyclic shearing, making the specimen less affected by cyclic loading times. This resulted in reinforced RSM's dynamic characteristics being more stable than those of unreinforced RSM. 3) Geocell reinforcement caused the degradation rate of the maximum shear modulus of RSM to decrease with increasing rubber content, and to increase with increasing vertical pressure. In addition, the influence of geocell reinforcement on the normalized shear modulus degradation curves was significant up to 20% rubber content.

Author statement

Mengtao Wu: Methodology, Formal analysis, Investigation, Writing – original draft.

Wenhui Tian: Investigation, Data curation.

Fangcheng Liu: Conceptualization, Methodology, Project administration, Funding acquisition.

Jun Yang: Supervision, Writing – review & editing.

Declaration of competing interest

The authors declare that they have no known competing financial interests or personal relationships that could have appeared to influence the work reported in this paper.

Data availability

Data will be made available on request.

Acknowledgments

This research was sponsored by the Research Fund of Institute of Engineering Mechanics, China Earthquake Administration under Grant no. 2019D25, the Natural Science Foundation of Hunan Province under Grant no. 2020JJ6073, the Key Research Project of Hunan Provincial Department of Education under Grant no. 21A0357, and the Post-doctoral Foundation of The University of Hong Kong.

References

[1] Collins KJ, Jensen AC, Mallinson JJ, Roenelle V, Smith IP. Environmental impact assessment of a scrap tyre artificial reef. ICES (Int Counc Explor Sea) J Mar Sci 2002;59(suppl):S243–9.
[2] Liu L, Cai G, Zhang J, Liu X, Liu K. Evaluation of engineering properties and environmental effect of recycled waste tire-sand/soil in geotechnical engineering: a compressive review. Renew Sustain Energy Rev 2020;126:109831.
[3] Shrestha S, Ravichandran N, Raveendra M, Attenhofer JA. Design and analysis of retaining wall backfilled with shredded tire and subjected to earthquake shaking. Soil Dynam Earthq Eng 2016;90:227–39.
[4] Ecemis N, Valizadeh H, Karaman M. Sand-granulated rubber mixture to prevent liquefaction-induced uplift of buried pipes: a shaking table study. Bull Earthq Eng 2021;19(7):2817–38.
[5] Liu L, Li Z, Cai G, Zhang J, Dai B. Long-term performance of temperature and humidity in the road embankment constructed with recycled construction and demolition wastes. J Clean Prod 2022;356:131851.
[6] Wu M, Liu F, Li Z, Bu G. Micromechanics of granulated rubber–soil mixtures as a cost-effective substitute for geotechnical fillings. Mech Adv Mater Struct 2022: 1–17.
[7] Anbazhagan P, Manohar DR. Energy absorption capacity and shear strength characteristics of waste tire crumbs and sand mixtures. Int J Geotech Earthq Eng 2015;6(1):28–49.
[8] Tsang HH. Seismic isolation by rubber–soil mixtures for developing countries. Earthq Eng Struct Dynam 2008;37(2):283–303.
[9] Tsang HH, Pitilakis K. Mechanism of geotechnical seismic isolation system: analytical modeling. Soil Dynam Earthq Eng 2019;122:171–84.
[10] Feng ZY, Sutter KG. Dynamic properties of granulated rubber/sand mixtures. Geotech Test J 2000;23(3):338–44.
[11] Shang SP, Sui XX, Zhou ZJ. Study of dynamic shear modulus of granulated rubber-sand mixture. Rock Soil Mech 2010;31(2):377–81 [In Chinese].
[12] Senetakis K, Anastasiadis A, Pitilakis K. Dynamic properties of dry sand/rubber (SRM) and gravel/rubber (GRM) mixtures in a wide range of shearing strain amplitudes. Soil Dynam Earthq Eng 2012;33(1):38–53.
[13] Nakhaei A, Marandi SM, Kermani SS, Bagheripour MH. Dynamic properties of granular soils mixed with granulated rubber. Soil Dynam Earthq Eng 2012;43: 124–32.
[14] Anastasiadis A, Senetakis K, Pitilakis K. Small-strain shear modulus and damping ratio of sand-rubber and gravel-rubber mixtures. Geotech Geol Eng 2012;30(2): 363–82.
[15] Anbazhagan P, Manohar DR. Small-to large-strain shear modulus and damping ratio of sand-tyre crumb mixtures. In: Geo-Chicago 2016; 2016. p. 305–15.
[16] Sarajpoor S, Kavand A, Zogh P, Ghalandarzadeh A. Dynamic behavior of sand-rubber mixtures based on hollow cylinder tests. Construct Build Mater 2020;251: 118948.
[18] Liu FC, Chen Lu, Wang HD. Evaluation of dynamic shear modulus and damping ratio of rubber-sand mixture based on cyclic simple shear tests. Rock Soil Mech 2016;37(7):1903–13 [In Chinese)].
[17] Anbazhagan P, Manohar DR, Rohit D. Influence of size of granulated rubber and tyre chips on the shear strength characteristics of sand–rubber mix. Geomechanics Geoengin 2017;12(4):266–78.
[19] Ding Y, Zhang J, Chen X, Wang X, Jia Y. Experimental investigation on static and dynamic characteristics of granulated rubber-sand mixtures as a new railway subgrade filler. Construct Build Mater 2021;273:121955.
[20] Xiong W, Li Y. Seismic isolation using granulated tire–soil mixtures for less-developed regions: experimental validation. Earthq Eng Struct Dynam 2013;42 (14):2187–93.
[21] Manohar DR, Anbazhagan P. Shear strength characteristics of geosynthetic reinforced rubber-sand mixtures. Geotext Geomembranes 2021;49(4):910–20.
[22] Liu FY, Ying MJ, Yuan GH, Wang J, Ni JF. Particle shape effects on the cyclic shear behavior of the soil–geogrid interface. Geotext Geomembranes 2021;49(4): 991–1003.
[23] Morsy AM, Zornberg JG, Leshchinsky D, Christopher BR, Han J, Tanyu BF. Experimental evaluation of the interaction among neighboring reinforcements in geosynthetic-reinforced soils. J Geotech Geoenviron Eng 2020;146(10):04020107.
[24] ASTM D 422-63. Standard Test Method for Particle-Size Analysis of Soils. 2002. Reapproved.
[25] Darendeli MB. Development of a New Family of Normalized Modulus Reduction and Material Damping Curves. The university of Texas at Austin; 2001.
[26] Wei X, Chen Y, Yang J. A unified critical state constitutive model for cyclic behavior of silty sands. Comput Geotech 2020;127:103760.